This article has an erratum available at: https://dx.doi.org/10.21037/cdt-2022-1 and the article has been update on 2022-08-15 at here.

Original Article

# MicroRNA-155 inhibition attenuates myocardial infarction-induced connexin 43 degradation in cardiomyocytes by reducing pro-inflammatory macrophage activation

**Hai-Tao Yang[1#], Li-Li Li[2#], Song-Nan Li[3], Jin-Tao Wu[1], Ke Chen[1], Wei-Feng Song[1], Guo-Bao Zhang[1], Ji-Fang Ma[1], Hai-Xia Fu[1], Sheng Cao[4], Chuan-Yu Gao[1], Juan Hu[1]**

[1]Heart Center of Henan Provincial People's Hospital, Central China Fuwai Hospital, Central China Fuwai Hospital of Zhengzhou University, Zhengzhou, China; [2]Central Laboratory, Renmin Hospital of Wuhan University, Wuhan, China; [3]Department of Cardiology, Beijing Anzhen Hospital, Capital Medical University, Beijing Institute of Heart Lung and Blood Vessel Diseases, Beijing, China; [4]Department of Ultrasound, Renmin Hospital of Wuhan University, Wuhan, China

*Contributions:* (I) Conception and design: J Hu, CY Gao, JF Ma, WF Song; (II) Administrative support: JF Ma, WF Song; (III) Provision of study materials or patients: LL Li, HX Fu; (IV) Collection and assembly of data: HT Yang, S Cao, K Chen; (V) Data analysis and interpretation: GB Zhang, SN Li, JT Wu; (VI) Manuscript writing: All authors; (VII) Final approval of manuscript: All authors.

[#]These authors contributed equally to this work.

*Correspondence to:* Juan Hu; Chuan-Yu Gao. Heart Center of Henan Provincial People's Hospital, Central China Fuwai Hospital, Central China Fuwai Hospital of Zhengzhou University, Zhengzhou 450003, China. Email: 1429695430@qq.com; gaocy6802@163.com.

**Background:** Degradation of pro-inflammatory macrophage-mediated connexin 43 (Cx43) plays an important role in post-myocardial infarction (MI) arrhythmogenesis, microRNA (miR)-155 produced by macrophages has been shown to mediate post-MI effects. We hypothesized that miR-155 inhibition attenuated MI-induced Cx43 degradation by reducing pro-inflammatory macrophage activation.

**Methods:** MI was induced by permanent ligation of the left anterior descending coronary artery in male C57BL/6 mice. Lipopolysaccharide (LPS)-stimulated mice bone marrow-derived macrophages (BMDMs) and hypoxia-induced neonatal rat cardiomyocytes (NRCMs) were used *in vitro* models. qRT-PCR, Western-blot and immunofluorescence were used to analyze relevant indicators.

**Results:** The expression levels of miR-155, interleukin-1 beta (IL-1β), and matrix metalloproteinase (MMP)7 were higher in MI mice and LPS-treated BMDMs than in the sham/control groups, treatment with a miR-155 antagomir reversed these effects. Moreover, miR-155 inhibition reduced ventricular arrhythmias incidence and improved cardiac function in MI mice. Cx43 expression was decreased in MI mice and hypoxia-exposed NRCMs, and hypoxia-induced Cx43 degradation in NRCMs was reduced by application of conditioned medium from LPS-induced BMDMs treated with the miR-155 antagomir, but increased by conditioned medium from BMDMs treated with a miR-155 agomir. Importantly, NRCMs cultured in conditioned medium from LPS-induced BMDMs transfected with small interfering RNA against IL-1β and MMP7 showed decreased hypoxia-mediated Cx43 degradation, and this effect also was diminished by BMDM treatment with the miR-155 agomir. Additionally, siRNA-mediated suppressor of cytokine signaling 1 (SOCS1) knockdown in LPS-induced BMDMs promoted Cx43 degradation in hypoxia-exposed NRCMs, and the effect was reduced by the miR-155 inhibition.

**Conclusions:** MiR-155 inhibition attenuated post-MI Cx43 degradation by reducing macrophage-mediated IL-1β and MMP7 expression through the SOCS1/nuclear factor-κB pathway.

**Keywords:** Myocardial infarction (MI); ventricular arrhythmias; connexin 43 (Cx43); microRNA-155 (miR-55)

Submitted Dec 01, 2021. Accepted for publication Jun 01, 2022.

doi: 10.21037/cdt-21-743

**View this article at:** https://dx.doi.org/10.21037/cdt-21-743

## Introduction

Ventricular arrhythmias and sudden death are major complications of myocardial infarction (MI) (1), and connexin 43 (Cx43) degradation has been identified as a key molecular mechanism contributing to these adverse outcomes (2). Studies have confirmed that Cx43 protein is mainly present in ventricular cardiomyocytes and is degraded in ischemic cardiomyopathy (3,4). Additionally, Cx43 knockout mice exhibit slowed conduction and an increased likelihood of arrhythmia (5). Thus, inhibition of Cx43 degradation represents a promising therapeutic strategy for reducing MI-induced ventricular arrhythmias and sudden death.

Studies in animal and human models have demonstrated that pro-inflammatory macrophages significantly impact inflammation-mediated remodeling and arrhythmia development following MI (6,7). Consistently, after MI in mice, matrix metalloproteinase (MMP)7 and interleukin-1 beta (IL-1β) produced post-MI by pro-inflammatory macrophages induce Cx43 degradation, which is closely related to the pathological process of MI-induced arrhythmia (8-10). Interestingly, the nuclear factor κB (NF-κB) pathway activation promotes the secretion of IL-1β and MMP7 by pro-inflammatory macrophages (11,12). Therefore, the inactivation of pro-inflammatory macrophages could theoretically attenuate post-MI Cx43 degradation by reducing NF-κB pathway-related expression of IL-1β and MMP7.

MicroRNA (miR)-155 exerts important effects in the inflammatory, immunity, infection and differentiation (13). Previous studies have revealed that roles and effects of miR-155 in the various heart diseases via various targets (14-18). Importantly, miR-155 produced by pro-inflammatory macrophages promotes cardiac fibrosis and hypertrophy in a paracrine manner with suppressor of cytokine signaling 1 (SOCS1) as its target (15,19,20). Our recent research also showed that the SOCS1/NF-κB axis exerts vital effects in miR-155-mediated post-MI sympathetic neural remodeling and cardiomyocyte apoptosis via the regulation of pro-inflammatory macrophages (21,22). However, it is unknown whether miR-155 inhibition can decrease the pro-inflammatory macrophage-derived IL-1β and MMP7 expression levels and lead to further degradation of Cx43 post-MI via the SOCS1/NF-κB axis. We therefore hypothesized that the upregulation of miR-155 can result in increased Cx43 degradation and susceptibility to ventricular arrhythmias after MI due to increases in pro-inflammatory macrophage-mediated IL-1β and MMP7 expression. We tested this hypothesis through a series of *in vivo* and *in vitro* experiments, and the results provide insight into potential targets for reducing the risk of ventricular arrhythmias after MI. We present the following article in accordance with the ARRIVE reporting checklist (available at https://cdt.amegroups.com/article/view/10.21037/cdt-21-743/rc).

## Methods

### *Reagents and antibodies*

Murine macrophage colony-stimulating factor (M-CSF) was purchased from PeproTech (Rocky Hill, NJ, USA); lipopolysaccharide (LPS) was purchased from Sigma-Aldrich (Merck KGaA, Darmstadt, Germany; l2630). Antibody sources were as follows: anti-phospho (p)-P65, anti-p-inhibitor of kBα (IkBα), anti-SOCS1, anti-MMP7, and anti-Cx43 antibodies were obtained from Cell Signaling Technology (Danvers, MA, USA); anti-IL-1β and anti-glyceraldehyde 3-phosphate dehydrogenase (GAPDH) were purchased from Abcam (Cambridge, UK); and horseradish peroxidase (HRP)-conjugated anti-rabbit IgG was obtained from Amersham Biosciences (Buckinghamshire, UK). The control con/miR-155-agomir, con/miR-155-antagomir (scrambled sequence), miR-155 antagomir (a 2'-O-methyl + 5' cholesterol-modified miR-155 inhibitor), small interfering (si)RNA control, and siRNAs specific for SOCS1, IL-1β, and MMP7 were purchased from Guangzhou RiboBio Co., Ltd. (Guangzhou, China).

### *Animals*

The study procedures were approved by the Institutional Animal Care and Use Committee at the Third People's Hospital of Wuhan (Date 7 August 2020/No. SY2020-001), and was carried out in accordance with the Guide for the Care and Use of Laboratory Animals published by the US National Institutes of Health (8th Edition, NRC 2011). A protocol was prepared before the study without registration. Total 64 healthy male C57BL/6 mice (weighing 24–26 g) were housed (12 h light/dark cycle) with food and water available ad libitum purchased from Hubei Provincial Disease Control Center. For surgery, the mice were anesthetized with sodium pentobarbital (50 mg/kg, Sigma-Aldrich) and constant ventilation was maintained (respiratory depression was observed but unexpected, hypothermia and food intake were not observed). Occlusion

 

of the left anterior descending artery was used to induced MI model, regional cyanosis of the myocardial surface and ST segment elevation of the electrocardiogram (ECG) were confirmed as successful MI procedure, as previously described (23). Animals were randomly assigned including the following four groups of mice according to randomization sequences by using a computer-based random order generator: (I) the sham group (the animal experimental number/total number 10/12) mice underwent sham operation without the left anterior descending artery ligation; (II) the MI group (the animal experimental number/total number 12/18); (III) the MI + con-antagomir group (the animal experimental number/total number 11/18); and (IV) the MI + miR-155 antagomir group (the animal experimental number/total number 12/16). Before surgery, the mice in the sham group and MI group received an injection of saline through the tail vein, whereas mice in the MI + con-antagomir group and MI + miR-155 antagomir group received tail vein injections of 80 mg/kg miR-155 antagomir and the same amount of con-antagomir for consecutive 3 days before left anterior descending artery occlusion following a previously described method (24), euthanasia was performed one week after MI.

### *Culture and transfection of adult mouse bone marrow-derived macrophages (BMDMs)*

As previously described (21,22), BMDMs from mouse femurs and tibias were isolated and cultured in RPMI-1640 complete medium with M-CSF (50 ng/mL). BMDMs were transfected separately with 100 nM of either miR-155 con-agomir/agomir, miR-155 con-antagomir/antagomir, SOCS1 con-siRNA/siRNA, IL-1β con-siRNA/siRNA, or MMP7 con-siRNA/siRNA using Lipofectamine 2000 (Invitrogen, Thermo Fisher Scientific, Waltham, MA, USA) according to the manufacturer's instructions. The conditioned medium and cells from transfected BMDMs were used in further assays.

### *Preparation of neonatal rat cardiomyocytes (NRCMs)*

Ventricular NRCMs, derived from 1- to 3-day-old rats, were isolated and then cultured in hypoxic conditions ($CO_2$:$N_2$:$O_2$ at a ratio of 94:5:1) as described previously (25).

### *Quantitative reverse transcription polymerase chain reaction (qRT-PCR)*

As previously described (26), RNA was extracted using TRIzol (15596–018, Invitrogen) and transcribed into complementary DNAs (cDNAs) using the PrimeScript RT Reagent Kit (RR037A, Takara Bio Inc., Shiga, Japan). The sequences of the primers: (I) miR-155: reverse transcription (RT) 5'-GTCGTATCCAGTGCGTGTCGTGGAG TCGGCAATTGCACTGGATACGACACCCCT-3', forward 5'-GGGGGTTAATGCTAATTGTGAT-3' and reverse 5'-AGTGCGTGTCGTGG-3'; (II) U6: RT 5'-CGCTTCACGAATTTGCGTGTCAT-3', forward 5'-GCTTCGGCAGCACATATACTAAAAT-3' and reverse 5'-CGCTTCACG AATTTGCGTGTCAT-3'; (III) inducible nitric oxide synthase (iNOS): forward 5'-TTGGCTCCAGCATGTACCCT-3' and reverse 5'-TCCTGCCCACTGAGTTCGTC-3'; and (IV) GAPDH: forward 5'-ATGGGTGTGAACCACGAGA-3' and reverse 5'-CAGGGATGATGTTCTGGGCA-3'.

### *Western blot analysis*

Tissue samples were collected from the peri-infarct and infarct zones of mouse hearts post-MI at 1 week and from the same cardiac tissue zones of mice in the sham group at 1 week. The proteins were separated by sodium dodecyl sulfate polyacrylamide gel electrophoresis and transferred to polyvinylidene difluoride membranes. After the blots were incubated overnight with primary antibodies (anti-p-P65, anti-p-IκBα, anti-SOCS1, anti-MMP7, anti-Cx43, anti-IL-1β, and anti-GAPDH), the membranes were washed and incubated with secondary antibody (HRP-goat anti-rabbi; HRP-goat anti-mouse) incubation. The blots were developed using an enhanced chemiluminescence kit, and band intensities were quantified using a Bio-Rad imaging system (Hercules, CA, USA). The relative band intensity for each protein of interest was normalized to that from the sham control group, which was set at a value of 1 (100%).

### *Immunofluorescence*

As previously described (27,28), tissues were fixed and slices were used for immunohistochemical analysis. Firstly,

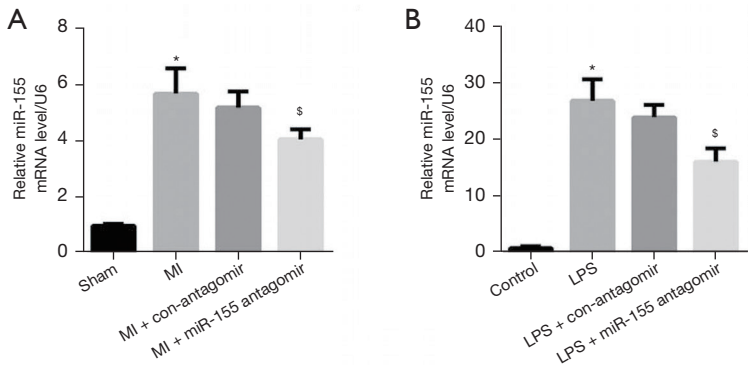


**Figure 1** MiR-155 level in cardiac tissue of a mouse MI model and in LPS-induced BMDMs. (A) MiR-155 level in cardiac tissue following MI in mice (n=5; *, P<0.01 *vs.* the sham control group; $, P<0.05 *vs.* the MI group). (B) MiR-155 level in BMDMs after 24 h of treatment with LPS (n=3; *, P<0.01 *vs.* the control group; $, P<0.05 *vs.* the LPS group). U6 small nuclear RNA was used as an internal control. Con, control; MI, myocardial infarction; LPS, lipopolysaccharide; BMDMs, bone-marrow-derived macrophages.

the slices were incubated with anti-iNOS and anti-Cx43 antibody overnight at 4 ℃, and then were incubated with a fluorescein isothiocyanate (FITC)-conjugated secondary antibody, and finally counterstained with DAPI. Fluorescence images were captured using an Olympus BX51 microscope (Olympus Corporation, Tokyo, Japan), and Image pro-plus was used to analyze.

### *Langendorff perfusion and ventricular arrhythmia inducibility*

As described previously (29), mouse hearts were collected and perfused through a Langendorff system. Briefly, the hearts were quickly excised and hung on the Langendorff-perfusion system (AD Instruments, Bella Vista, NSW, Australia). Hearts that did not recover the regular spontaneous rhythm or had irreversible myocardial ischemia were not subjected to electrophysiology testing. To trigger ventricular arrhythmia in the peri-infarct region, burst pacing (2-ms pulses at 50 Hz, 2-s burst duration) was repeated 20 times with 2-s intervals. we defined ventricular arrhythmia as rapid ventricular contractions lasting for at least 2 s, non-sustained ventricular arrhythmia as contractions lasting for 2–30 s, and sustained ventricular arrhythmia as contractions lasting for more than 30 s (30).

### *Cardiac function*

Echocardiography with a Mylab30CV (Esaote S.p.A.) instrument and a 10-MHz linear array ultrasound transducer was used to evaluate left ventricle cardiac function in mice at 1 week post-MI. Data included: left ventricle end-diastolic dimension (LVEDD), left ventricle end-systolic dimension (LVESD), left ventricle ejection fraction (LVEF), and left ventricle fractional shortening (LVFS).

### *Statistical analysis*

All data are expressed as mean ± standard deviation (SD). The independent sample Student's *t*-test was used to evaluate significant differences between two groups, and one-way analysis of variance (ANOVA) was used to evaluate significant differences multi-group comparisons. The data analysis was performed using SPSS 20 software. and P<0.05 was considered statistically significant

## Results

### *MiR-155 expression was upregulated in mouse cardiac tissue after MI and in LPS-induced BMDMs*

Comparison of miR-155 level in cardiac tissues of mice in various groups by qRT-PCR revealed that miR-155 level was obviously upregulated in the MI group compared to the sham group (P<0.01), while this effect was partially lowered by inhibiting miR-155 (P<0.05; *Figure 1A*). Moreover, upregulation of miR-155 was also observed in LPS-treated BMDMs compared with control BMDMs (P<0.01), but this effect was partially reduced by inhibiting miR-155 (P<0.05; *Figure 1B*). These changes in miR-155 expression in both MI mice and LPS-treated BMDMs were consistent with

 

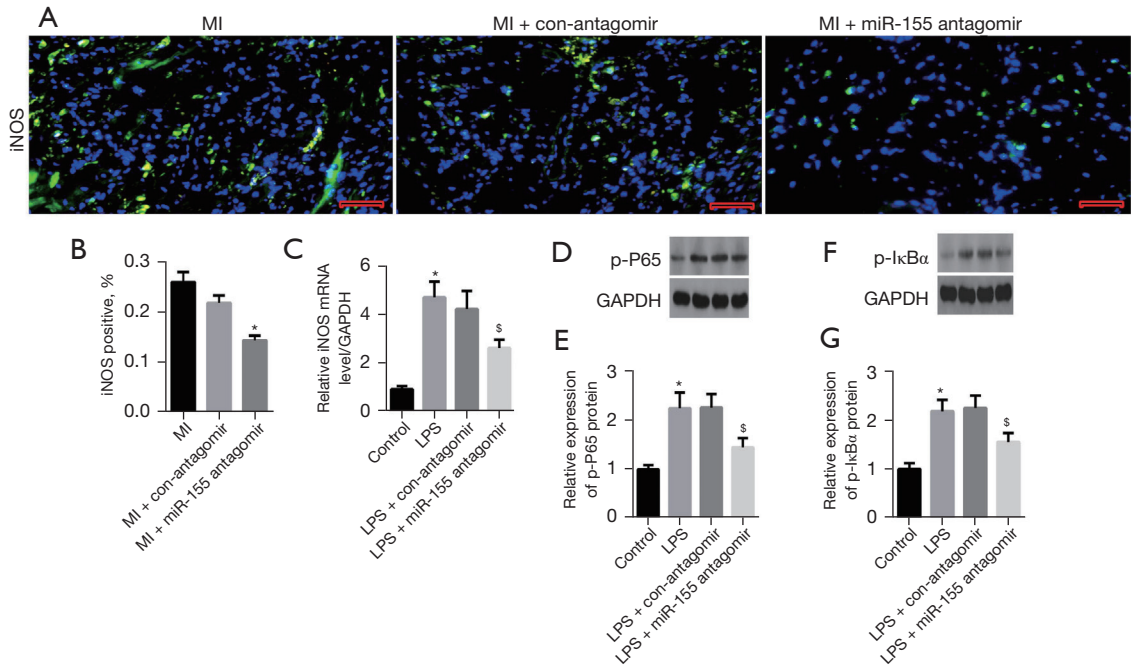


**Figure 2** Effects of miR-155 inhibition on MI- and LPS-induced macrophage polarization and NF-κB pathway *in vivo* and *in vitro*. (A) Representative photomicrographs of iNOS expression (green staining). Nuclei were counterstained with DAPI. Scale bar 20 μm. (B) The percentage of iNOS positive cells in cardiac tissue of mice following MI induction (n=5; *, P<0.05 *vs.* the MI group). (C) mRNA expression of iNOS in LPS-induced BMDMs with or without miR-155 antagomir treatment (n=3; *, P<0.01 *vs.* the control group; $, P<0.05 *vs.* the LPS group). (D,F) Representative Western blots of p-P65 and p-IκBα expression in LPS-induced BMDMs with or without miR-155 antagomir treatment for 24 h. (E,G) Quantitative analysis of data in D and F, respectively (n=3; *, P<0.01 *vs.* the control group; $, P<0.05 *vs.*the LPS group). Con, control; iNOS, inducible nitric oxide synthase; MI, myocardial infarction; LPS, lipopolysaccharide; BMDMs, bone-marrow-derived macrophages; NF-κB, nuclear factor κB.

our observations in previous studies (21,22).

### *MiR-155 inhibition attenuated MI- and LPS-induced macrophage polarization and NF-κB pathway activation*

Pro-inflammatory macrophage polarization was tested in the infarct area of mouse hearts by immunofluorescence staining for the established marker iNOS. The numbers of iNOS-positive cells were similar between the MI + con-antagomir and MI groups, whereas the number of iNOS-positive cells was lower in the MI + miR-155 antagomir group than in the MI group (*Figure 2A*,2B; P<0.05).

To investigate the effect of miR-155 on macrophage polarization and NF-κB pathway activation *in vitro*, we cultured BMDMs with or without LPS/miR-155 con-antagomir/miR-155 antagomir. The results showed that iNOS mRNA expression was significantly upregulated in the LPS group compared with control group (P<0.01), but this upregulation was attenuated by miR-155 inhibition (P<0.05; *Figure 2C*). Considering that NF-κB pathway activation promotes M1 macrophage polarization (31), we also investigated the effect of miR-155 on NF-κB pathway in LPS-treated BMDMs. We found that the upregulation of p-IκBα and p-P65 proteins induced by LPS BMDMs was significantly diminished by miR-155 antagomir treatment (P<0.05; *Figure 2D-2G*). These findings suggest that miR-155 promotes macrophage polarization and NF-κB pathway activation following MI.

### *MiR-155 inhibition attenuated MI- and LPS-induced IL-1β and MMP7 expression*

Because IL-1β and MMP7 play important roles in MI-induced ventricular arrhythmias, we explored the effects of miR-155 on IL-1β and MMP7 expression *in vivo* and *in vitro* by Western blot analyses. At 1-week post-MI in

 

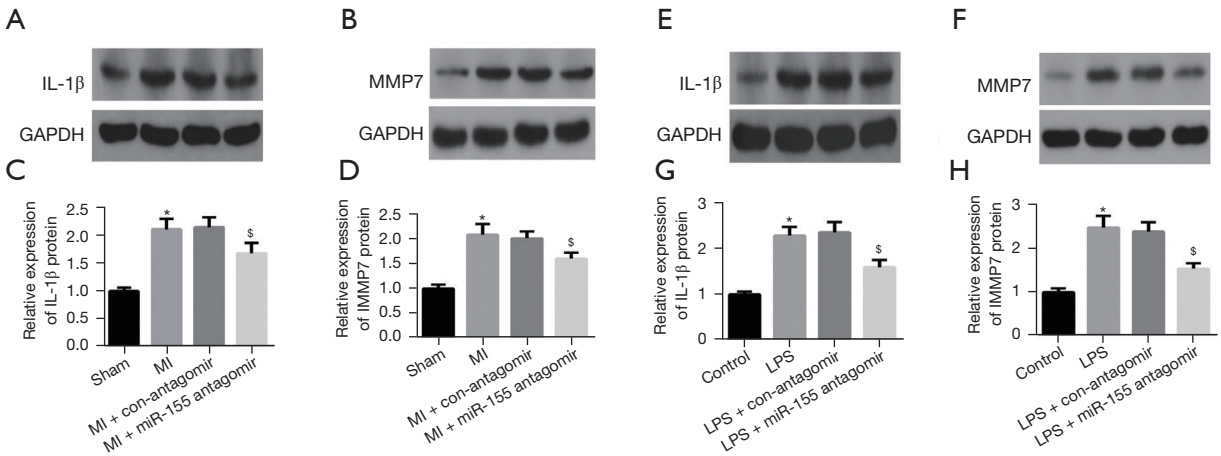


**Figure 3** Effects of miR-155 inhibition on MI- and LPS-induced IL-1β and MMP7 expression *in vivo* and *in vitro*. (A,B) Representative Western blots of IL-1β and MMP7 expression in cardiac tissue following MI. (C,D) Quantitative analysis of data in (A) and (B), respectively (n=5; *, P<0.01 *vs.* the sham group; $, P<0.05 *vs.* the MI group). (E,F) Representative Western blots of IL-1β and MMP7 expression in LPS-induced BMDMs with or without miR-155 antagomir treatment for 24 h. (G,H) Quantitative analysis of data in (E) and (F), respectively (n=3; *, P<0.01 *vs.* the control group; $, P<0.05 *vs.* the LPS group). Con, control; MI, myocardial infarction; LPS, lipopolysaccharide; BMDMs, bone-marrow-derived macrophages; IL-1β, interleukin-1β; MMP7, matrix metalloproteinase 7.

mice, IL-1β and MMP7 protein expression was substantially increased in the infarcted heart tissue of mice in the MI group compared with levels in cardiac tissue from the sham mice (both P<0.01). However, these increases in IL-1β and MMP7 protein expression were attenuated by miR-155 inhibition (P<0.05; *Figure 3A-3D*).

Based upon research showing that IL-1β and MMP7 are mainly secreted by M1 macrophages (9,10,32), we investigated the effects of miR-155 expression on IL-1β and MMP7 production by LPS-induced BMDMs. Consistent with the results from our animal experiment, we found that LPS significantly upregulated IL-1β and MMP7 expression compared with levels in control cells, but treatment with the miR-155 antagomir significantly decreased LPS-induced IL-1β and MMP7 expression in BMDMs (both P<0.05; *Figure 3E-3H*).

Together, our *in vivo* results indicate that inhibition of miR-155 attenuated MI-induced upregulation of IL-1β and MMP7, and the *in vitro* experiment suggests this upregulation was mediated via NF-κB signaling.

### *MiR-155 inhibition attenuated MI-induced Cx43 degradation*

Cx43 expression in the peri-infarct border zone of the mouse heart at 1-week post-MI was assessed by immunofluorescence staining and Western blotting. The density of cells stained positively for Cx43 was significantly diminished post-MI, but miR-155 inhibition decreased CX43 degradation induced by MI (*Figure 4A*). Western blot analysis confirmed these differences Cx43 expression in cardiac tissue post-MI with and without miR-155 antagomir treatment (P<0.05; *Figure 4B,4C*).

To investigate the mechanism by which miR-155 influences Cx43 degradation post-MI, we cultured hypoxic-induced NRCMs with conditioned medium from LPS-induced BMDMs with or without miR-155 antagomir/agomir to evaluate Cx43 expression. We observed that Cx43 expression was obviously decreased in hypoxic group compared to control group, importantly, Cx43 expression was significantly increased in hypoxic-induced NRCMs cultured in conditioned medium from LPS-induced macrophages treated with the miR-155 antagomir compared with treated with miR-155 con-antagomir. However, conditioned medium from LPS-induced BMDMs treated with miR-155 agomir had the opposite effect on Cx43 expression in hypoxia-induced NRCMs (P<0.05; *Figure 4D-4I*). These findings indicate that miR-155 derived from BMDMs regulates hypoxia-induced Cx43 degradation in NRCMs via a paracrine manner.

Previous studies have confirmed that IL-1β and MMP7 play an important role in MI-induced Cx43 degradation

 

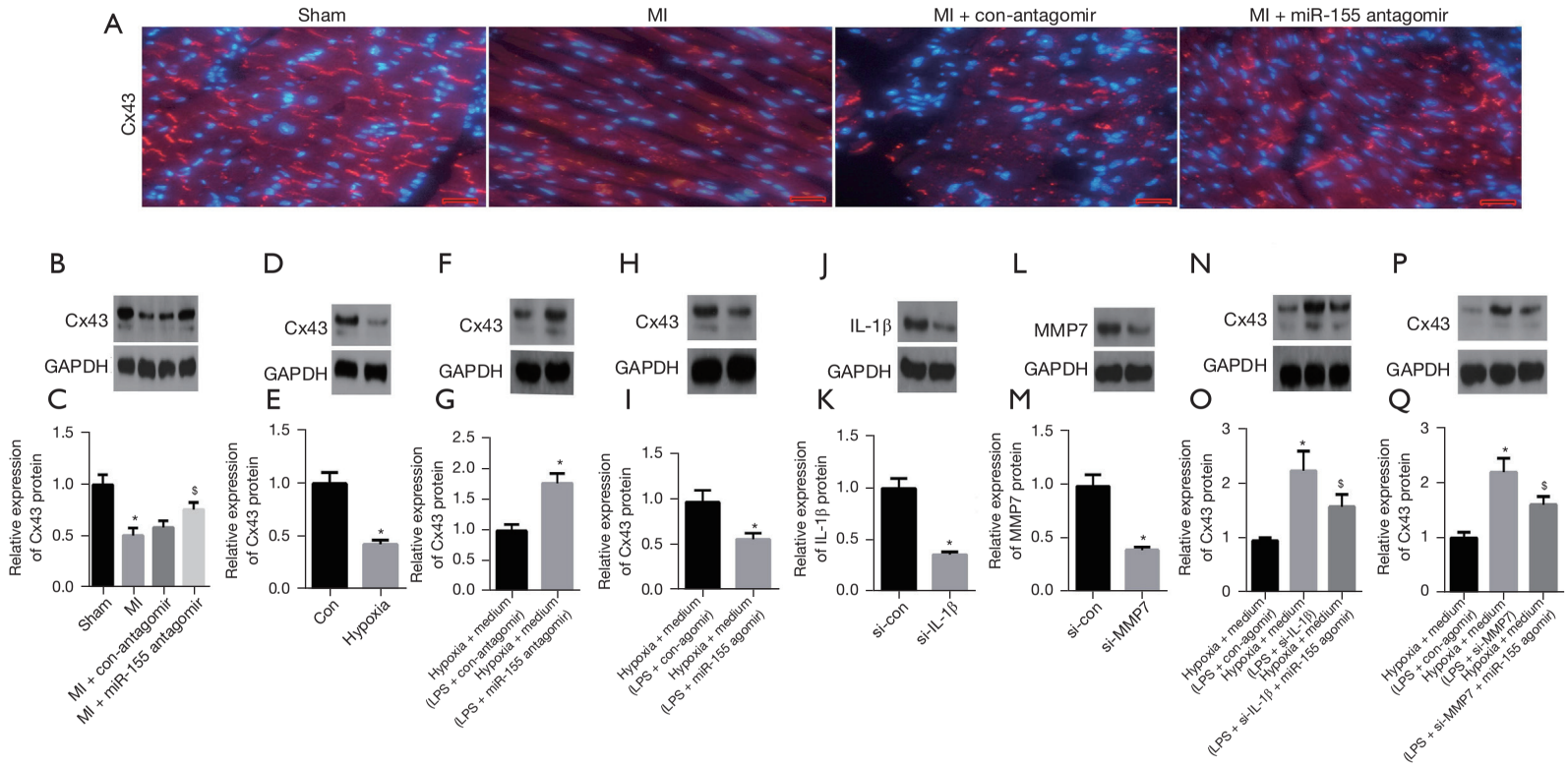


**Figure 4** Effect of miR-155 inhibition on Cx43 degradation *in vivo* post-MI and *in vitro* in hypoxic NRCMs. (A) Representative photomicrographs of Cx43 expression (red staining) in mouse cardiac tissue after MI. Nuclei were counterstained with DAPI. Scale bar, 20 μm. (B) Representative Western blots of Cx43 expression in mouse cardiac tissue after MI. (C) Quantitative analysis of data in (B) (n=5; *, P<0.01 *vs.* the sham group; $, P<0.05 *vs.* the MI group). (D-I) Conditioned medium was obtained from LPS-induced BMDMs treated with or without miR-155 antagomir/agomir for 24 h and then applied to cultures of hypoxia-induced NRCMs for 24 h. (D,F,H) Representative Western blots of Cx43 expression. (E,G,I) Quantitative densitometric analysis of data from (D), (F) and (H), respectively [n=3; *, P<0.05 *vs.* the Con, the hypoxia + medium (LPS + con-antagomir/con-agomir) or the hypoxia + medium (LPS + miR-155 con-agomir) group]. (J-Q) LPS-induced BMDMs were treated with or without si-IL-1β RNA, si-MMP7 RNA or miR-155 agomir for 24 h, and the resulting conditioned medium was applied to hypoxia-induced NRCMs for 24 h. (J,L,N,P) Representative Western blots of IL-1β, MMP7 and Cx43 expression. (K,M,O,Q) Quantitative densitometric analysis of data from (J), (L), (N) and (P), respectively [n=3; *, P<0.05 *vs.* the si-con or the hypoxia + medium (LPS + con-agomir) group; $, P<0.05 *vs.* the hypoxia + medium (LPS + si-IL-1β or LPS + si-MMP7) group]. Con, control; Cx43, connexin 43; MI, myocardial infarction; LPS, lipopolysaccharide; BMDMs, bone-marrow-derived macrophages; NRCMs, neonatal mouse cardiomyocytes; IL-1β, interleukin-1β; MMP7, matrix metalloproteinase 7.

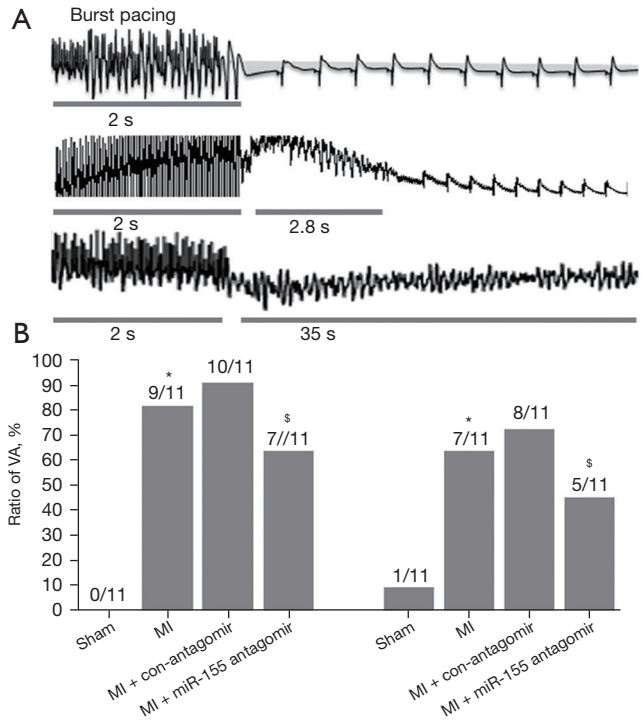


**Figure 5** Effect of miR-155 inhibition on MI-induced VA. Langendorff perfusion was performed on hearts prepared from mice of the sham, MI, MI + con-antagomir, and MI + miR-155 antagomir groups. (A) Representative VA induced by burst-pacing stimulations. (B) Comparison of non-sustained/sustained VA inducibility rates (*, P<0.05 *vs.* the sham group; $, P<0.05 *vs.* the MI group). Con, control; MI, myocardial infarction; VA, ventricular arrhythmia.

(8-10). To further clarify how miR-155 regulates Cx43 expression in NRCMs, we transfected BMDMs with siRNAs against IL-1β and MMP7 and examined whether miR-155-mediated Cx43 degradation in hypoxic NRCMs was dependent on IL-1β and MMP7 produced by pro-inflammatory macrophages. The results showed that expression of IL-1β and MMP7 was obviously decreased in siRNA-IL-1β/siRNA-MMP7 group compared with si-control group (P<0.01; *Figure 4J-4M*), Cx43 expression was significantly upregulated in hypoxia-induced NRCMs exposed to conditioned medium from LPS-induced BMDMs transfected with IL-1β or MMP7 siRNA compared with the expression level in hypoxic NRCMs in conditioned medium from BMDMs without IL-1β or MMP7 silencing. However, treatment of the transfected LPS-induced BMDMs with miR-155 agomir significantly reversed this effect (P<0.05; *Figure 4N-4Q*). Taken together, these data indicate that miR-155 induces Cx43 degradation in hypoxic NRCMs by promoting IL-1β and MMP7 expression by pro-inflammatory macrophages.

### *MiR-155 inhibition suppressed MI-induced ventricular arrhythmias and cardiac dysfunction in mice*

Next, we evaluated whether miR-155 is involved in ventricular arrhythmias induced by MI via applying the Langendorff-perfusion system to the mouse MI model. The ratio of non-sustained ventricular arrhythmias and sustained ventricular arrhythmias was obviously increased in the MI group and MI + con-antagomir group, with no significant difference observed between these two groups (P>0.05). Importantly, compared to the MI group, the ratio of non-sustained ventricular arrhythmias and sustained ventricular arrhythmias was significantly decreased in the MI + miR-155-antagomir group (P<0.05; *Figure 5*), indicating that miR-155 participates in post-MI ventricular arrhythmias. Additionally, evaluation of cardiac function post-MI in mice at 1 week revealed reductions in LVEF and LVFS and increases in LVEDD and LVESD in the MI group compared with the sham group. However, inhibition of miR-155 significantly reversed these effects (P<0.05; *Figure 6*).

 

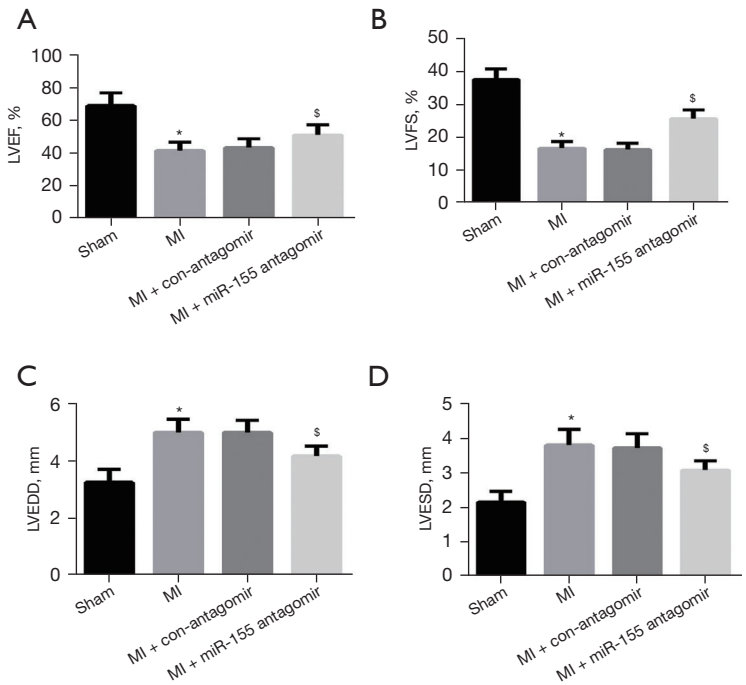


**Figure 6** Effect of miR-155 inhibition on post-MI cardiac dysfunction. (A-D) Representative echocardiographic findings after MI or sham operation in mice of the sham, MI, MI + con-antagomir, and MI + miR-155 antagomir groups (n=7; *, P<0.01 *vs.* the sham control group; $, P<0.05 *vs.* the MI group). Con, control; MI, myocardial infarction; LVEF, left ventricular ejection fraction; LVFS, left ventricular fractional shortening; LVEDD, left ventricular end-diastolic diameter; LVESD, left ventricular end-systolic diameter.

These results indicate that miR-155 inhibition improved cardiac dysfunction after MI.

### *MiR-155 inhibition attenuated Cx43 degradation by augmenting SOCS1 expression in LPS-induced BMDMs*

To further elucidate the mechanism by which miR-155 influences Cx43 degradation post-MI, we investigated the involvement of the miR-155 target gene *SOCS1*. First, Western blotting confirmed the upregulated expression of SOCS1 in LPS-induced BMDMs (P<0.01; *Figure 7A*,*7B*), and addition of the miR-155 antagomir resulted in even higher SOCS1 expression in these cells (P<0.05). We then transfected LPS-induced BMDMs with SOCS1 siRNA and confirmed the reduced expression of SOCS1 by Western blotting (P<0.01; *Figure 7C*,*7D*). We found that Cx43 expression was obviously decreased in hypoxic group compared to control group (P<0.01; *Figure 7E*,*7F*), interestingly, conditioned medium from these BMDMs transfected with si-SOCS1 compared with the expression level in hypoxic NRCMs in conditioned medium from BMDMs without si-SOCS1led to a significant reduction in Cx43 expression in hypoxic NRCMs, and this effect was reversed by addition of the miR-155 antagomir to the BMDMs before conditioned medium collection (P<0.05; *Figure 7G*,*7H*). Together, these results demonstrate that pro-inflammatory macrophage-derived miR-155 promotes Cx43 degradation in cardiomyocytes, at least in part, via the downregulation of SOCS1 in pro-inflammatory macrophages (*Figure 8*).

## Discussion

In the present investigation of the effect of miR-155 on MI-induced Cx43 degradation, we first confirmed that miR-155 level was significantly increased in post-MI cardiac tissue and LPS-induced BMDMs. Then through a series of *in vivo* and *in vitro* experiments, we determined that inhibition of miR-155 attenuated Cx43 degradation in cardiac tissue post-MI and in cultured hypoxia-induced cardiomyocytes by decreasing pro-inflammatory macrophage-derived IL-1β and MMP7 expression via the SOCS1/NF-κB pathway. Overall, these findings indicate that miR-155 contributes to post-MI arrhythmias by

 

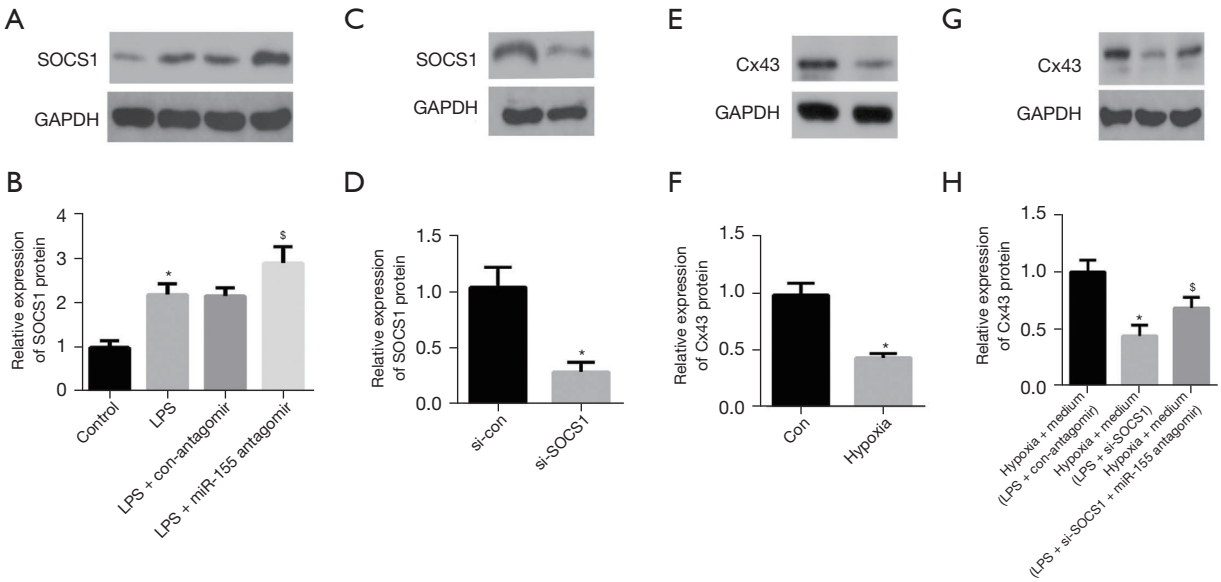


**Figure 7** Involvement of SOCS1 expression in LPS-induced BMDMs in the effect of miR-155 inhibition on Cx43 degradation in cardiomyocytes. (A,B) Representative Western blots (A) and quantitative analysis (B) of SOCS1 treated with or without miR-155 antagomir in LPS-induced BMDMs for 24 h (n=3; *, P<0.01 *vs.* the control group; $, P<0.05 *vs.* LPS group). (C,D) Representative Western blot (C) and quantification analysis (D) of SOCS1 in BMDMs transfected with si-control or si-SOCS1 (n=3; *, P<0.01 *vs.* the si-con group). (E-H) Conditioned medium was collected from LPS-induced BMDMs treated with or without miR-155 antagomir or si-SOCS1 for 24 h and then applied to hypoxia-induced NRCMs for 24 h. (E,G) Representative Western blots of Cx43 expression. (F,H) Quantitative analysis of data from (E) and (G), respectively [n=3; *, P<0.01 *vs.* the Con or the hypoxia + medium (LPS + con-antagomir) group; $, P<0.05 *vs.* the hypoxia + medium (LPS + si-SOCS1) group]. Con, control; MI, myocardial infarction; LPS, lipopolysaccharide; BMDMs, bone-marrow-derived macrophages; NRCMs, neonatal mouse cardiomyocytes; SOCS1, suppressor of cytokine signaling 1.

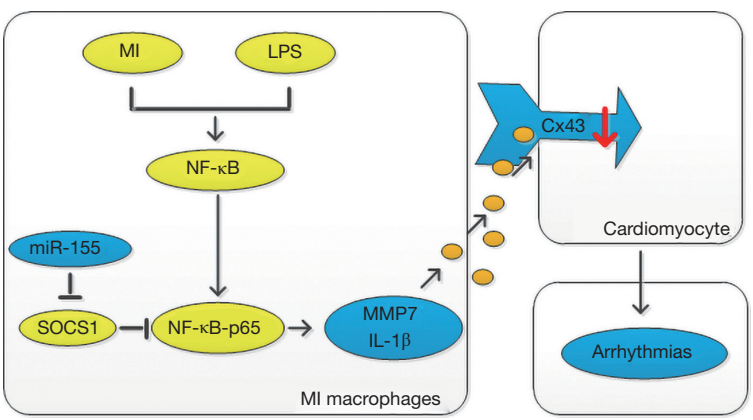


**Figure 8** Summary of the roles of miR-155 in the MI-induced connexin 43 degradation in cardiomyocytes by activating pro-inflammatory macrophage activation. MI, myocardial infarction; LPS, lipopolysaccharide; SOCS1, suppressor of cytokine signaling 1; IL-1β, interleukin-1β; MMP7, matrix metalloproteinase 7; NF-κB, nuclear factor κB.

promoting the degradation of Cx43.

MiR-155 has been significantly upregulated in activated macrophages, T cells, and B cells, and it is known to play important roles in cell apoptosis, inflammation, immunity and infection (13). Several studies have showed that miR-155 is mainly produced by pro-inflammatory macrophages (19,20) and has been confirmed to participate in various cardiovascular diseases (15,17,19,33,34). Presently, the data showed that miR-155 expression was prominently increased in the cardiac tissue of MI mice as well as in LPS-induced BMDMs, on the contrary, miR-155 inhibition decreased iNOS (M1 macrophage markers), p-IκBα and p-P65 expression, consistent with the findings of our previous study (21,22). These results highlight that miR-155 promotes post-MI pro-inflammatory macrophage polarization and NF-κB pathway activation. Interesting, many studies have reported that miR/miR and miR/long non-coding RNA (lncRNA) can regulate each other and eventually lead to various pathological changes. For example, amnion membrane alleviates LPS-induced cardiomyocyte injury via upregulation of miR-21 and miR-146, and exerts an important effect on miR-155-mediated inflammatory cytokine expression (35). Additionally, lncRNA/miR-155/IKKi signaling axis modulates pathological cardiac hypertrophy (36) and lncRNA MALAT1/miR-155/IL-10 axis induces tolerogenic dendritic cells and regulatory T cells (36). However, whether miR-155 antagomir affects miR-155 expression to further regulate other miR/lncRNA expression levels and participates in related pathological processes will be explored in our further experiments. Research has shown that pro-inflammatory macrophages are recruited to the infarct site where they promote inflammatory factor expression and further regulate cardiomyocyte function in a paracrine manner, influencing the incidence post-MI ventricular arrhythmias by mediating NF-κB pathway activation (37-40). Specifically, high levels of IL-1β produced by pro-inflammatory macrophages in cardiac tissue post-MI have been implicated in this cell-cell uncoupling and shown to slow conduction via degradation of Cx43 (8,10,41). Additionally, pro-inflammatory macrophages in the infarct zone express MMP7, which also has been reported to induce Cx43 degradation and attenuate conduction (9,42). Our results revealed that miR-155 inhibition reduced MI/LPS-induced upregulation of IL-1β and MMP7 levels in BMDMs. Importantly, myocardial Cx43 expression is known to be reduced in mice after MI as well as in patients with ischemic heart disease (43,44), and degradation of Cx43 is an established pathological mechanism for ventricular arrhythmias and sudden cardiac death after MI (45). Notably, Cx43 degradation in the post-MI heart is distinctly observed in areas of macrophage infiltration (10,46), and studies have confirmed the involvement of pro-inflammatory macrophages in MI-induced inflammation, which results in Cx43 degradation (47,48). However, it remained unclear whether miR-155 in pro-inflammatory macrophages influences the expression levels of IL-1β and MMP7 to further promote post-MI Cx43 protein degradation. We demonstrated that inhibiting of miR-155 attenuated MI/hypoxia-induced cardiomyocytes Cx43 degradation and also showed that overexpression of miR-155 had opposite effect. Moreover, siRNA-mediated knockdown of IL-1β and MMP7 in pro-inflammatory macrophages diminished the hypoxia-mediated degree of Cx43 degradation in cardiomyocytes, and these effects were antagonized by treatment of the macrophages with miR-155 agomir, suggesting that miR-155 produced by pro-inflammatory macrophages regulates cardiomyocyte Cx43 degradation in a paracrine manner.

Recent research has shown that inhibiting miR-155 attenuates atrial fibrillation by targeting CACNA1C (49). To further demonstrate the role of miR-155 in ventricular arrhythmias induced by MI, we examined the incidence of ventricular arrhythmias in MI model mice by miR-155 antagomir treatment and found that miR-155 inhibition reduced the incidence of ventricular arrhythmias. Moreover, miR-155 inhibition improved post-MI cardiac dysfunction, and these findings are in line with a previous report (19). These effects of miR-155 on cardiac dysfunction may be related to the relevant changes in IL-1β and MMP7 expression in pro-inflammatory macrophages. IL-1β expression has been linked with post-MI cardiac dysfunction by research showing that inhibition of post-MI IL-1β signaling improved cardiac function and reduced the incidence of heart failure, and another study reported that MMP7 may influence post-MI left ventricle remodeling (50-52). In the present study, the mechanisms for the improvements in post-MI cardiac function with miR-155 inhibition may be, at least in part, related to decreased expression of IL-1β and MMP7 in pro-inflammatory macrophages, leading to attenuated Cx43 degradation. It has been reported that Cx43 degradation promotes deterioration of cardiac function (53,54), and our data demonstrate that miR-155 antagomir exerted a regulatory effect on Cx43 degradation and improved cardiac function. However, if the expression of Cx43 is altered in mice with MI treated with miR-155 antagomir, it may better explain

 

whether miR-155 regulates the expression of Cx43 and then regulates cardiac dysfunction. This topic will be further explored in our subsequent experiments.

SOCS1, a target of miR-155, inactivates NF-κB pathway in pro-inflammatory macrophages (21,22). Thus, we hypothesized that the effect of miR-155 on Cx43 degradation is related to SOCS1 expression in BMDMs. Our results demonstrated that miR-155 inhibition promoted SOCS1 expression in LPS-stimulated BMDMs, whereas SOCS1 knockdown in these cells significantly increased hypoxia-induced Cx43 degradation in cardiomyocytes. Moreover, this effect was reversed by treatment of the macrophages with the miR-155 antagomir, these data indicate that SOCS1 is an important target in miR-155-mediated Cx43 degradation, our data indicate a crucial role for SOCS1 in the control of the miR-155-mediated Cx43 degradation. Moreover, highlights of this manuscript are as follows: (I) miR-155 inhibition attenuated post-MI Cx43 degradation of cardiomyocytes by decreasing pro-inflammatory macrophage-derived IL-1β and MMP7 expression; (II) SOCS1/NF-κB signaling pathway played an important role at least in part in the miR-155-mediated IL-1β and MMP7 expression; (III) miR-155 inhibition reversed the development of ventricular arrhythmias and cardiac dysfunction in MI mice by attenuating post-MI the degradation of Cx43.

In conclusion, our study revealed that miR-155 increases IL-1β and MMP7 expression by pro-inflammatory macrophages, which results in the degradation of Cx43 in cardiomyocytes via paracrine signaling and further contributes to the development of ventricular arrhythmias and cardiac dysfunction in MI mice. Additionally, these effects of miR-155 are mediated, at least in part, via SOCS1/NF-κB signaling.

## Conclusions

Overall, our findings suggest that miR-155 participates in the pathophysiology of ventricular arrhythmia and cardiac dysfunction induced by MI via promoting the degradation of Cx43 in cardiomyocytes via an increasing pro-inflammatory macrophage activation.

## Acknowledgments

*Funding:* This work was supported by the Joint Construction Project of Medical Science and Technology of Henan Province (Grant Nos. LHGJ20200072, LHGJ20200071 and LHGJ20200077) and the Medical Science and Technology Project of Henan Province (No. SBGJ202002030).

## Footnote

*Reporting Checklist:* The authors have completed the ARRIVE reporting checklist. Available at https://cdt.amegroups.com/article/view/10.21037/cdt-21-743/rc

*Data Sharing Statement:* Available at https://cdt.amegroups.com/article/view/10.21037/cdt-21-743/dss

*Conflicts of Interest:* All authors have completed the ICMJE uniform disclosure form (available at https://cdt.amegroups.com/article/view/10.21037/cdt-21-743/coif). All authors report that this work was supported by the Joint Construction Project of Medical Science and Technology of Henan Province (Grant Nos. LHGJ20200072, LHGJ20200071 and LHGJ20200077) and the Medical Science and Technology Project of Henan Province (No. SBGJ202002030). The authors have no other conflicts of interest to declare.

*Ethical Statement:* The authors are accountable for all aspects of the work in ensuring that questions related to the accuracy or integrity of any part of the work are appropriately investigated and resolved. The study protocol was approved by the Institutional Animal Care and Use Committee at the Third People's Hospital of Wuhan (date 7 August 2020/No. SY2020-051). Ethical approval was firstly obtained from own institutions (date 18 June 2020//No. WDRM-20200606), but the number of animal rooms in our hospitals was limited, ethical approval was again obtained from Wuhan Third People's Hospital and animals were fed in the animal room of Wuhan Third People's Hospital. We confirm that no one from Third People's Hospital of Wuhan participated in our study. We only used the animal room of Wuhan Third People's Hospital to raise animals, including animal husbandry, animal model establishment and related animal experimental data acquisition, other experiments are carried out in our own laboratory. The animal study was carried out in Wuhan Third People's Hospital and Renmin Hospital of Wuhan University), and the study was carried out in accordance with the Guide for the Care and Use of Laboratory Animals published by the US National Institutes of Health (8th Edition, NRC 2011).



 

## References

1. Rosso R, Hochstadt A, Viskin D, et al. Polymorphic ventricular tachycardia, ischaemic ventricular fibrillation, and torsade de pointes: importance of the QT and the coupling interval in the differential diagnosis. Eur Heart J 2021;42:3965-75.
2. Xiao S, Shimura D, Baum R, et al. Auxiliary trafficking subunit GJA1-20k protects connexin-43 from degradation and limits ventricular arrhythmias. J Clin Invest 2020;130:4858-70.
3. Michela P, Velia V, Aldo P, et al. Role of connexin 43 in cardiovascular diseases. Eur J Pharmacol 2015;768:71-6.
4. Severs NJ, Bruce AF, Dupont E, et al. Remodelling of gap junctions and connexin expression in diseased myocardium. Cardiovasc Res 2008;80:9-19.
5. Gutstein DE, Morley GE, Tamaddon H, et al. Conduction slowing and sudden arrhythmic death in mice with cardiac-restricted inactivation of connexin43. Circ Res 2001;88:333-9.
6. Hulsmans M, Clauss S, Xiao L, et al. Macrophages Facilitate Electrical Conduction in the Heart. Cell 2017;169:510-522.e20.
7. Peet C, Ivetic A, Bromage DI, et al. Cardiac monocytes and macrophages after myocardial infarction. Cardiovasc Res 2020;116:1101-12.
8. De Jesus NM, Wang L, Lai J, et al. Antiarrhythmic effects of interleukin 1 inhibition after myocardial infarction. Heart Rhythm 2017;14:727-36.
9. Lindsey ML, Escobar GP, Mukherjee R, et al. Matrix metalloproteinase-7 affects connexin-43 levels, electrical conduction, and survival after myocardial infarction. Circulation 2006;113:2919-28.
10. De Jesus NM, Wang L, Herren AW, et al. Atherosclerosis exacerbates arrhythmia following myocardial infarction: Role of myocardial inflammation. Heart Rhythm 2015;12:169-78.
11. Laczko R, Chang A, Watanabe L, et al. Anti-inflammatory activities of Waltheria indica extracts by modulating expression of IL-1B, TNF-α, TNFRII and NF-κB in human macrophages. Inflammopharmacology 2020;28:525-40.
12. Gao Y, Nan X, Shi X, et al. SREBP1 promotes the invasion of colorectal cancer accompanied upregulation of MMP7 expression and NF-κB pathway activation. BMC Cancer 2019;19:685.
13. Cao RY, Li Q, Miao Y, et al. The Emerging Role of MicroRNA-155 in Cardiovascular Diseases. Biomed Res Int 2016;2016:9869208.
14. He W, Huang H, Xie Q, et al. MiR-155 Knockout in Fibroblasts Improves Cardiac Remodeling by Targeting Tumor Protein p53-Inducible Nuclear Protein 1. J Cardiovasc Pharmacol Ther 2016;21:423-35.
15. Heymans S, Corsten MF, Verhesen W, et al. Macrophage microRNA-155 promotes cardiac hypertrophy and failure. Circulation 2013;128:1420-32.
16. Marques FZ, Vizi D, Khammy O, et al. The transcardiac gradient of cardio-microRNAs in the failing heart. Eur J Heart Fail 2016;18:1000-8.
17. Nazari-Jahantigh M, Wei Y, Noels H, et al. MicroRNA-155 promotes atherosclerosis by repressing Bcl6 in macrophages. J Clin Invest 2012;122:4190-202.
18. Biros E, Moran CS, Wang Y, et al. microRNA profiling in patients with abdominal aortic aneurysms: the significance of miR-155. Clin Sci (Lond) 2014;126:795-803.
19. Wang C, Zhang C, Liu L, et al. Macrophage-Derived mir-155-Containing Exosomes Suppress Fibroblast Proliferation and Promote Fibroblast Inflammation during Cardiac Injury. Mol Ther 2017;25:192-204.
20. Corsten MF, Papageorgiou A, Verhesen W, et al. MicroRNA profiling identifies microRNA-155 as an adverse mediator of cardiac injury and dysfunction during acute viral myocarditis. Circ Res 2012;111:415-25.
21. Hu J, Huang CX, Rao PP, et al. Inhibition of microRNA-155 attenuates sympathetic neural remodeling following myocardial infarction via reducing M1 macrophage polarization and inflammatory responses in mice. Eur J Pharmacol 2019;851:122-32.
22. Hu J, Huang CX, Rao PP, et al. MicroRNA-155 inhibition attenuates endoplasmic reticulum stress-induced cardiomyocyte apoptosis following myocardial infarction via reducing macrophage inflammation. Eur J Pharmacol 2019;857:172449.
23. Li L, Weng Z, Yao C, et al. Aquaporin-1 Deficiency Protects Against Myocardial Infarction by Reducing Both Edema and Apoptosis in Mice. Sci Rep 2015;5:13807.
24. Wang H, Bei Y, Huang P, et al. Inhibition of miR-155

 

Protects Against LPS-induced Cardiac Dysfunction and Apoptosis in Mice. Mol Ther Nucleic Acids 2016;5:e374.
25. Divanovic S, Trompette A, Petiniot LK, et al. Regulation of TLR4 signaling and the host interface with pathogens and danger: the role of RP105. J Leukoc Biol 2007;82:265-71.
26. Hwang KC, Park SY, Park SP, et al. Specific maternal transcripts in bovine oocytes and cleavaged embryos: identification with novel DDRT-PCR methods. Mol Reprod Dev 2005;71:275-83.
27. Hu C, Zhang X, Song P, et al. Meteorin-like protein attenuates doxorubicin-induced cardiotoxicity via activating cAMP/PKA/SIRT1 pathway. Redox Biol 2020;37:101747.
28. Yin J, Wang Y, Hu H, et al. P2X7 receptor inhibition attenuated sympathetic nerve sprouting after myocardial infarction via the NLRP3/IL-1β pathway. J Cell Mol Med 2017;21:2695-710.
29. Qin M, Huang H, Wang T, et al. Absence of Rgs5 prolongs cardiac repolarization and predisposes to ventricular tachyarrhythmia in mice. J Mol Cell Cardiol 2012;53:880-90.
30. Wang D, Liu T, Shi S, et al. Chronic Administration of Catestatin Improves Autonomic Function and Exerts Cardioprotective Effects in Myocardial Infarction Rats. J Cardiovasc Pharmacol Ther 2016;21:526-35.
31. Yin H, Zhang X, Yang P, et al. RNA m6A methylation orchestrates cancer growth and metastasis via macrophage reprogramming. Nat Commun 2021;12:1394.
32. Mollenhauer M, Friedrichs K, Lange M, et al. Myeloperoxidase Mediates Postischemic Arrhythmogenic Ventricular Remodeling. Circ Res 2017;121:56-70.
33. Zhu J, Chen T, Yang L, et al. Regulation of microRNA-155 in atherosclerotic inflammatory responses by targeting MAP3K10. PLoS One 2012;7:e46551.
34. Seok HY, Chen J, Kataoka M, et al. Loss of MicroRNA-155 protects the heart from pathological cardiac hypertrophy. Circ Res 2014;114:1585-95.
35. Akseh S, Nemati M, Zamani-Gharehchamani E, et al. Amnion membrane proteins attenuate LPS-induced inflammation and apoptosis by inhibiting TLR4/NF-κB pathway and repressing MicroRNA-155 in rat H9c2 cells. Immunopharmacol Immunotoxicol 2021;43:487-94.
36. Yuan Y, Wang J, Chen Q, et al. Long non-coding RNA cytoskeleton regulator RNA (CYTOR) modulates pathological cardiac hypertrophy through miR-155-mediated IKKi signaling. Biochim Biophys Acta Mol Basis Dis 2019;1865:1421-7.
37. Wynn TA, Vannella KM. Macrophages in Tissue Repair, Regeneration, and Fibrosis. Immunity 2016;44:450-62.
38. Litviňuková M, Talavera-López C, Maatz H, et al. Cells of the adult human heart. Nature 2020;588:466-72.
39. Fujiu K, Nagai R. Contributions of cardiomyocyte-cardiac fibroblast-immune cell interactions in heart failure development. Basic Res Cardiol 2013;108:357.
40. Wang Y, Hu H, Yin J, et al. TLR4 participates in sympathetic hyperactivity Post-MI in the PVN by regulating NF-κB pathway and ROS production. Redox Biol 2019;24:101186.
41. Lyu J, Huang J, Wu J, et al. Lack of Macrophage Migration Inhibitory Factor Reduces Susceptibility to Ventricular Arrhythmias During the Acute Phase of Myocardial Infarction. J Inflamm Res 2021;14:1297-311.
42. Furman C, Copin C, Kandoussi M, et al. Rosuvastatin reduces MMP-7 secretion by human monocyte-derived macrophages: potential relevance to atherosclerotic plaque stability. Atherosclerosis 2004;174:93-8.
43. Peters NS, Coromilas J, Severs NJ, et al. Disturbed connexin43 gap junction distribution correlates with the location of reentrant circuits in the epicardial border zone of healing canine infarcts that cause ventricular tachycardia. Circulation 1997;95:988-96.
44. Martins-Marques T, Ribeiro-Rodrigues T, de Jager SC, et al. Myocardial infarction affects Cx43 content of extracellular vesicles secreted by cardiomyocytes. Life Sci Alliance 2020;3:e202000821.
45. Schulz R, Görge PM, Görbe A, et al. Connexin 43 is an emerging therapeutic target in ischemia/reperfusion injury, cardioprotection and neuroprotection. Pharmacol Ther 2015;153:90-106.
46. Peters NS. New insights into myocardial arrhythmogenesis: distribution of gap-junctional coupling in normal, ischaemic and hypertrophied human hearts. Clin Sci (Lond) 1996;90:447-52.
47. Westman PC, Lipinski MJ, Luger D, et al. Inflammation as a Driver of Adverse Left Ventricular Remodeling After Acute Myocardial Infarction. J Am Coll Cardiol 2016;67:2050-60.
48. Panizzi P, Swirski FK, Figueiredo JL, et al. Impaired infarct healing in atherosclerotic mice with Ly-6C(hi) monocytosis. J Am Coll Cardiol 2010;55:1629-38.
49. Wang J, Ye Q, Bai S, et al. Inhibiting microRNA-155 attenuates atrial fibrillation by targeting CACNA1C. J Mol Cell Cardiol 2021;155:58-65.
50. Ørn S, Ueland T, Manhenke C, et al. Increased interleukin-1β levels are associated with left ventricular

 

hypertrophy and remodelling following acute ST segment elevation myocardial infarction treated by primary percutaneous coronary intervention. J Intern Med 2012;272:267-76.
51. Sager HB, Heidt T, Hulsmans M, et al. Targeting Interleukin-1β Reduces Leukocyte Production After Acute Myocardial Infarction. Circulation 2015;132:1880-90.
52. Agnihotri R, Crawford HC, Haro H, et al. Osteopontin, a novel substrate for matrix metalloproteinase-3 (stromelysin-1) and matrix metalloproteinase-7 (matrilysin). J Biol Chem 2001;276:28261-7.
53. Dufeys C, Daskalopoulos EP, Castanares-Zapatero D, et al. AMPKα1 deletion in myofibroblasts exacerbates post-myocardial infarction fibrosis by a connexin 43 mechanism. Basic Res Cardiol 2021;116:10.
54. Rattka M, Westphal S, Gahr BM, et al. Spen deficiency interferes with Connexin 43 expression and leads to heart failure in zebrafish. J Mol Cell Cardiol 2021;155:25-35.

**Cite this article as:** Yang HT, Li LL, Li SN, Wu JT, Chen K, Song WF, Zhang GB, Ma JF, Fu HX, Cao S, Gao CY, Hu J. MicroRNA-155 inhibition attenuates myocardial infarction-induced connexin 43 degradation in cardiomyocytes by reducing pro-inflammatory macrophage activation. Cardiovasc Diagn Ther 2022;12(3):325-409. doi: 10.21037/cdt-21-743

 